Solid State Phenomena
ISSN: 1662-9779, Vol. 271, pp 76-84
doi:10.4028/www.scientific.net/SSP.271.76

Submitted: 2017-09-29
Revised: 2017-11-02
Accepted: 2017-11-20
Online: 2018-01-17

Reduction of 2,4-Dinitrophenol to 2,4-Diaminophenol Using AuNPs and AgNPs as Catalyst

Khongolzul Gerelbaatar[1,a], Ariunzaya Tsogoo[1,b], Rentsenmyadag Dashzeveg[1,c], Ninjbadgar Tsedev[2,d] and Erdene-Ochir Ganbold[3,e,*]

[1]Department of Chemistry, School of Arts and Sciences, National University of Mongolia, University street 1, Sukhbaatar district, Ulaanbaatar, 14201, Mongolia

[2]Department of Advanced Technology and Engineering, New Mongol Institute of Technology, Manlaibaatar Damdinsuren Street 43, Bayanzurkh district, Ulaanbaatar, 13330, Mongolia

[3]Department of Physics, School of Arts and Sciences, National University of Mongolia, University street 1, Sukhbaatar district, Ulaanbaatar, 14201, Mongolia

[a]khongoroo.0310@gmail.com, [b]ariuka4@gmail.com, [c]d_rentsenmyadag@num.edu.mn, [d]ninjts@yahoo.com, [e]erdeneochir_g@num.edu.mn

Keywords: nanoparticles, gold nanoparticles, silver nanoparticles, catalyst, 2,4-dinitrophenol, nitrophenols.

Abstract. In this study, colloidal metal nanoparticles have been prepared by the wet-chemical synthesis method. Gold and silver nanoparticles with approximate sphere shape were synthesized through the citrate-reduction method. The colloidal metal nanoparticles were characterized by using UV-vis absorption spectroscopy, photon cross-correlation spectroscopy (PCCS) and transmission electron microscope (TEM). Catalytic activities of the metal nanoparticles were investigated through reduction of 2,4-dinitrophenol to 2,4-diaminophenol in the presence of $NaBH_4$ at room temperature. Both gold and silver nanoparticles showed an excellent catalytic activity.

Introduction

Noble metal nanoparticles(e.g., Au, Ag, Pd, and Pt), in general, gold and silver nanoparticles, in particular, are very attractive because of their unique advantages, such as excellent robustness, stability, biocompatibility, and low-cost production with easy scale-up synthesis. In the past decades, due to their unique features like surface plasmon resonance, gold nanoparticles (AuNPs) have been potentially and practically applied in numerous fields such as catalysis [1], surface-enhanced Raman scattering (SERS) [2], biological sensing and imaging [3], diagnostics [4], photothermal therapy [5], and solar cells [6], while silver nanoparticles can be applied in a range of areas including plasmon resonance studies [7], anti-bacterial agents [8, 9], catalysis [10] and incorporated into products that range from photovoltaics to biological and chemical sensors.

One typical catalyzed reaction is reduction of aromatic nitro compounds by sodium borohydride to their corresponding amino derivatives, which has been used as model reaction, since it is easy to monitor with simple and fast analytical techniques without by-products [11, 12]. Moreover, nitrophenols are a kind of the most widely used industrial nitro aromatic compounds and frequently employed as intermediates in the production of explosives, pharmaceuticals, pesticides, pigments, dye, wood preservatives and rubber chemicals. Although, they are useful intermediates in the fabrication of various aforementioned materials, they also act as common environmental pollutants because of their toxicity and resistance to microbial degradation. Nitrophenols concentration in natural waters is restricted to less than 10 mg/l. [13]. For these reasons, in view of the green chemistry, reducing nitrophenols, a priority pollutant in the wastewater, to commercially important aminophenols is also very valuable. Up to date, various techniques such as membrane filtration, microbial degradation, photocatalytic degradation, electro-Fenton method, electrocoagulation, adsorption, electrochemical treatment and chemical reduction have been reported for removing

nitrophenols from contaminated water. Among these techniques, the chemical reduction of nitrophenols seems to be most efficient way to remove nitrophenols from waste contaminated water [14]. In previous researches, catalytic performance of gold nanoparticle [15] and silver nanoparticle [16] were evaluated in the reduction of 4-nitrophenol by $NaBH_4$. Xiao-Qiong Wu et al. have synthesized chitosan-Au hydrogel system via photoreduction and used it as reduction of nitrophenol derivatives by $NaBH_4$ [17]. However, catalytic performance of neither sphere gold nor silver nanoparticles have been evaluated through reduction of 2,4 -dinitrophenol (DNP), a derivative of aromatic nitro compounds, in the presence of $NaBH_4$. Only nickel particles decorated on electrospun polycaprolactone [18] and chitosan-Au hydrogel system [17] have been used for the reduction of DNP. In this research, catalytic activities of citrate-reduced metal nanoparticles were evaluated through the reduction of DNP.

Experimental Section

Materials. Hydrogen tetrachloroaurate (III) trihydrate ($HAuCl_4 \cdot 3H_2O$, Sigma-Aldrich, 99.9%), trisodium citrate dihydrate ($Na_3C_6H_5O_7 \cdot 2H_2O$, Sigma-Aldrich, 98%), silver nitrate ($AgNO_3$, Sigma-Aldrich), 2,4-dinitrophenol (Sigma-Aldrich), ethanol absolute (Unionlab, 99.99%) and sodium borohydride ($NaBH_4$, Nakarai Chemicals), were used without further purification.

Synthesis of Gold Nanoparticles. The colloidal dispersions of sphere shaped gold nanoparticles (AuNPs) were synthesized using the citrate reduction method [19]. 33 ml of 1 mM $HAuCl_4$ was preheated to boil in 50 ml beaker on the stirring plate. When it boiled, 3 ml of 1% sodium citrate as reducing agent was added to the vial under vigorous stirring. The solution was boiled on the stirring for another one hour. The level of solution was marked and concentration of solute was maintained by adding about 1 ml distilled water up to the drawn line, on the wall of the vial, in every 5 minutes. Then it was removed from the stirring plate and cooled down to the room temperature.

Synthesis of Silver Nanoparticles. The silver colloid nanoparticles were prepared by reduction of silver nitrate using sodium citrate [20]. 30 ml of 1 mM $AgNO_3$ was heated to boiling in 50 ml beaker on the stirring plate. To this solution, 1 ml of 1% trisodium citrate was added while the solution was mixed vigorously. The solution gradually turned pale yellow within a few minutes, indicating the formation of Ag nanoparticles. The solution was kept boiling for an additional 1h. Then it was removed from the heating and cooled to room temperature.

Characterization. Transmission electron microscopy (TEM) images of the metal nanoparticles were obtained using a JEOL JEM2100 HR. UV−vis absorption spectra were taken with the use of a UV2401-PC spectrophotometer. Particle size distribution analysis was performed using a NANOPHOX Sympetac GbmH. In order to evaluate the stability of the AuNPs, the spectrums of colloids with five different diluted concentrations were obtained by UV-vis spectrometer.

Catalytic Reaction Monitoring. The catalytic reduction of DNP was performed in a 1400 µl quartz spectrophotometer cuvette with a 10 mm optical path length and whole process was monitored by UV-vis absorption spectrophotometer. Before testing the catalytic activity of metal nanoparticles, we have to check if self-hydrolysis of $NaBH_4$ (Eq. 1) can reduce the DNP. For that reason, we performed three control experiments, in which the reductions of DNP was investigated in the presence of $NaBH_4$ and in the absence of metal catalyst. 10 µl of 0.01 M DNP ethanol solution was mixed with 890 µl of distilled water in the cuvette. Then cuvette was placed in the spectrophotometer and a curve was recorded. To initiate the reaction, 100 µl of 0.1 M freshly prepared $NaBH_4$ solution was added to the mixture. The whole process was monitored by UV-vis absorption spectrometer in the wavelength range of 200 to 800 nm with sampling interval of 1.0 nm at fast scan speed mode. Each spectrum was recorded in every 3 minutes.

$$NaBH_2 + 2H_2O \rightarrow NaBO_2 + 4H_2 \quad (1)$$

Secondly, reduction process was investigated in the presence of AuNPs to evaluate their catalytic activity. In the quartz cuvette 10 µl of 0.01 M DNP ethanol solution was mixed with 850 µl of

water, followed by the addition of 40 µl of 1 mM AuNPs colloids. After that cuvette was placed in the spectrophotometer and a first curve was recorded. Then, 100 µl of 0.1 M $NaBH_4$ solution was added into the mixture and reaction was initiated. The whole process was monitored by UV-vis absorption spectroscopy, and each spectrum was recorded in every 1.5 minutes for the first 30 minutes and once in 3 minutes until the end of the process.

Lastly, the catalytic activity of AgNPs was tested. The whole procedure was followed the procedure mentioned and 40 µl of 1mM AgNPs was used instead of AuNPs. The general catalytic reduction mechanism of 2,4-dinitrophenolate ion in aqueous solution is shown in Eq. 2.

$$BH_4^- + 2H_2O \rightarrow BO_2^- + 4H_2 \quad (2)$$

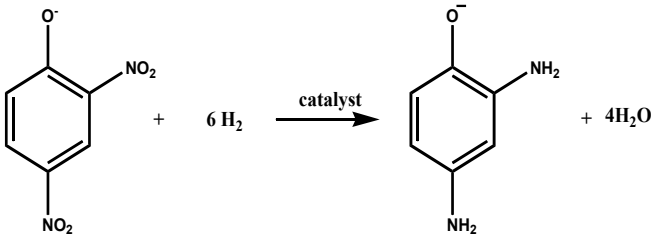

Results and Discussions

In Fig. 1, UV-vis spectrum of the AuNPs and AgNPs are shown where the surface plasmon resonance (SPR) absorption peaks were observed at 522 nm and 426 nm, respectively. The immobile wavelength of maximum absorbance through dilution indicated that AuNPs and AgNPs were stable at ambient temperature. Numbers in spectra indicate the total concentration of NPs in a diluted solutions.

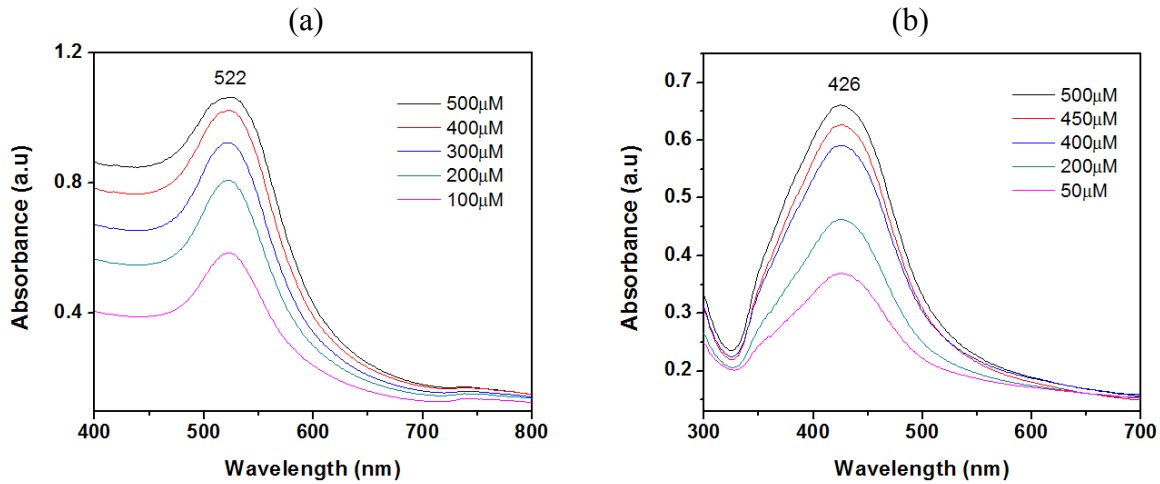

Fig. 1. UV−vis absorption spectrum of (a) AuNPs and (b) AgNPs.

Fig. 2 shows TEM images of as-synthesized nanoparticles which represent that nanoparticles have spherical shape.

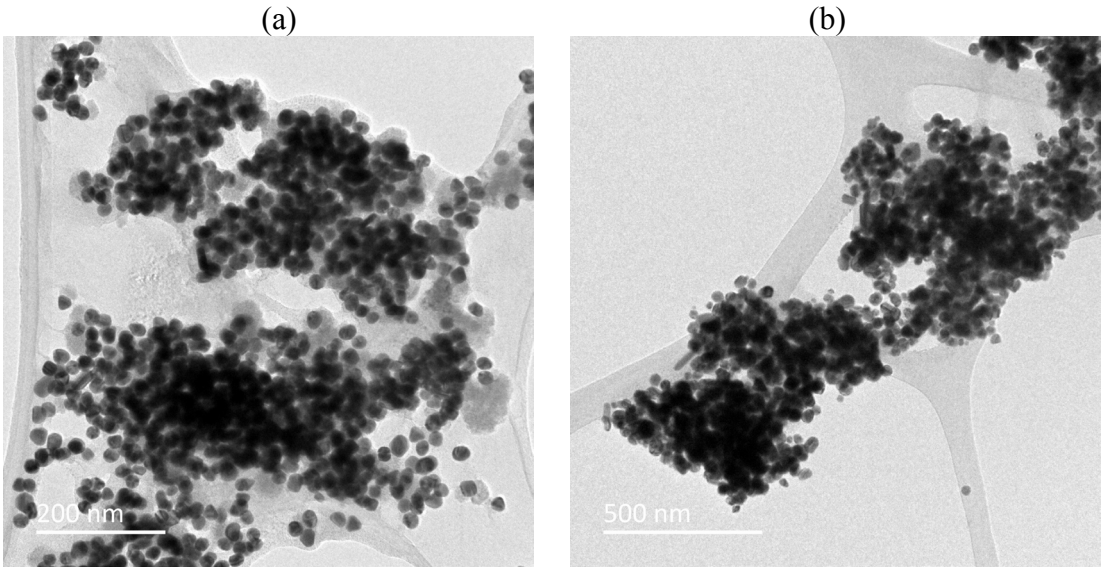

Fig. 2. TEM images of (a) AuNPs and (b) AgNPs.

Hydrodynamic diameter of the nanoparticles and their distribution analysis results were obtained on PCCS. The mean diameter of the particle with the highest distribution of AuNPs and AgNPs were 36.54 nm and 28.7 nm, respectively (Fig. 3).

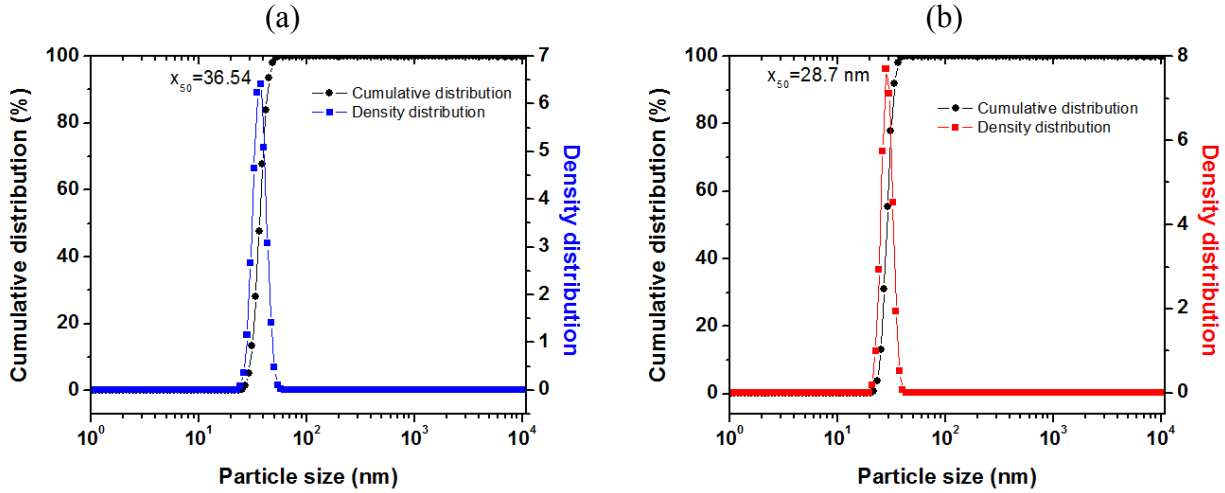

Fig. 3. PCCS spectra of (a) AuNPs and (b) AgNPs.

The catalytic reduction of toxic DNP to the corresponding aminophenol derivatives by $NaBH_4$ in the presence of gold and silver nanoparticles was selected as a model test reaction to examine the catalytic performance of our synthesized nanoparticles. By tracing and monitoring the location and intensity of the absorption peaks, the relative kinetic parameters were obtained.

The reaction without any nanoparticle was monitored by UV-vis spectrophotometer and spectra were recorded with 3 minutes intervals after addition of $NaBH_4$ (Fig. 4). DNP with $NaBH_4$ showed its strongest absorption peak at 355 nm as shown in Fig. 4. This peak was characterized as the electronic transition n-π*, owing to the lone pair of electrons (oxygen and nitrogen atoms) in the DNP structure. This peak was stable for one hour without any significant change showing that the reaction is unable without catalysis.

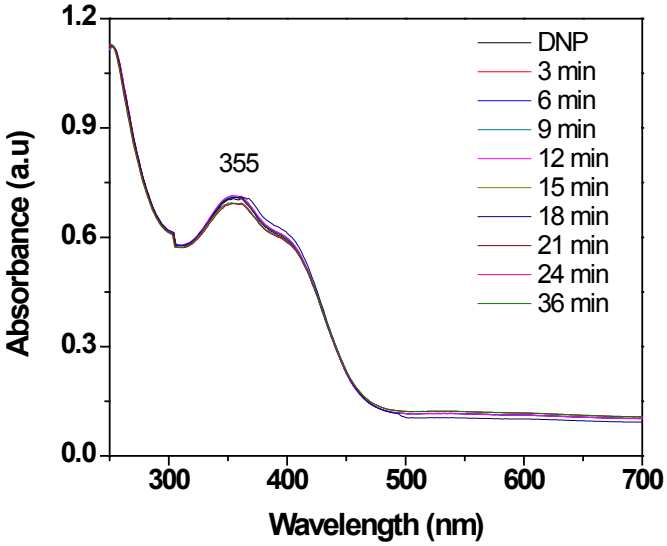

Fig. 4. Time-dependent UV-vis absorption spectrum for the reduction of DNP with $NaBH_4$ in the absence of metal nanoparticles.

After that the catalytic activity of AuNPs was analyzed by measuring the UV-vis spectrum of DNP in the presence of $NaBH_4$ and AuNPs in the range of 250-700 nm at various times. Within first 36 minutes the peak at 355 nm, slightly decreased which is due to decreased DNP concentration and new peaks appeared at 274 and 446 nm and kept increasing with reduction time. It indicated the formation of 2,4-dinitrophenolate ion in the reaction solution. The color of the solution transformed from yellow to pale orange. These new peaks showed their maximum absorption after 36 minutes as shown in Fig. 5.

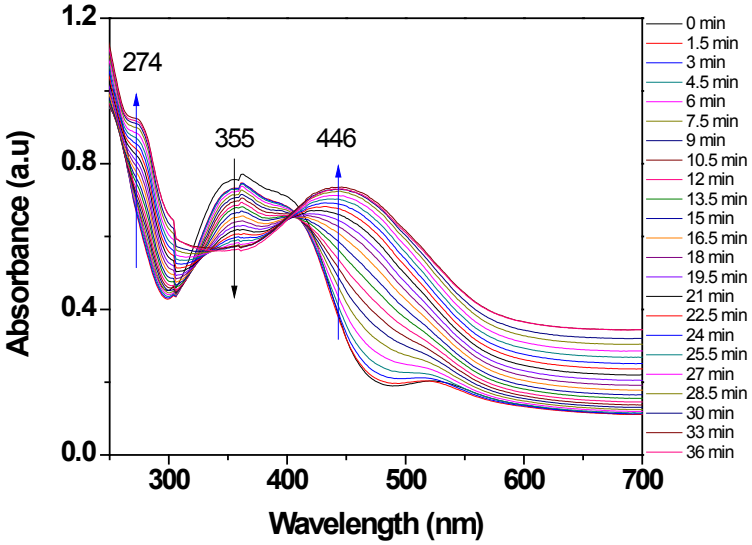

Fig. 5. Time-dependent UV-vis absorption spectrum for the reduction of DNP with $NaBH_4$ in the presence of AuNPs as a catalyst, first 36 minutes.

However, after around half hour from reaction starting, the intensities of absorptions at 274 nm and 446 nm gradually decreased as the reduction proceeds in the presence of AuNPs, shown in Fig. 6.

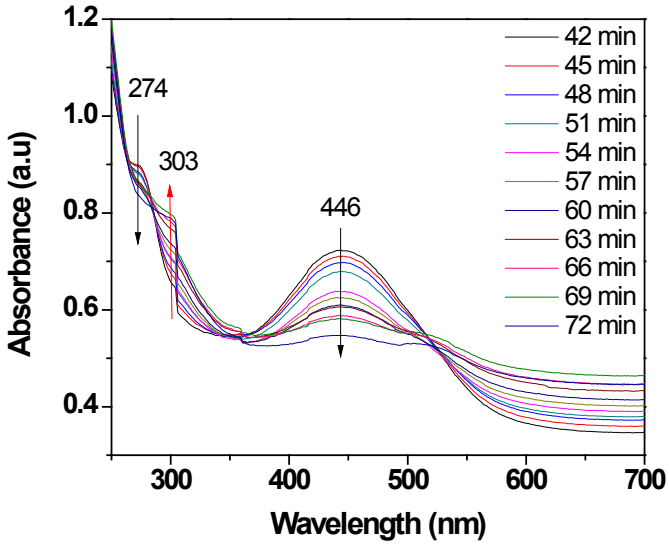

Fig. 6. Time-dependent UV-vis absorption spectrum for the reduction of DNP with $NaBH_4$ in the presence of AuNPs as a catalyst, last 30 minutes.

As 2,4-dinitrophenolate intermediate transformed into 2,4-diaminophenol (DAP), new small characteristic band around 303 nm was formed. Within the next 30 minutes, second half of the reaction process, the absorption bands of the DNP ion was totally disappeared and spectrum became stable as shown in Fig. 6. The reaction solution became colorless. This result is in agreement with the previous work by Kadir Karakas et al and Xiao-Qiong Wu et al. [18,19].

The catalytic activity of AgNPs was evaluated by measuring the UV-vis spectrum of DNP in the presence of $NaBH_4$ and AgNPs in the range of 250-600 nm at various times. Within first 15 minutes the peak at 355 nm slightly decreased and became stable which is due to decreased DNP concentration and new peaks appeared at 439 and 298 nm and kept increasing with reduction time. It indicated the formation of 2,4-dinitrophenolate ion and DAP in the reaction solution. The color of the solution transformed from yellow to pale orange. These new peaks showed their maximum absorption after 33 minutes, the first quarter of reaction time, shown in Fig. 7.

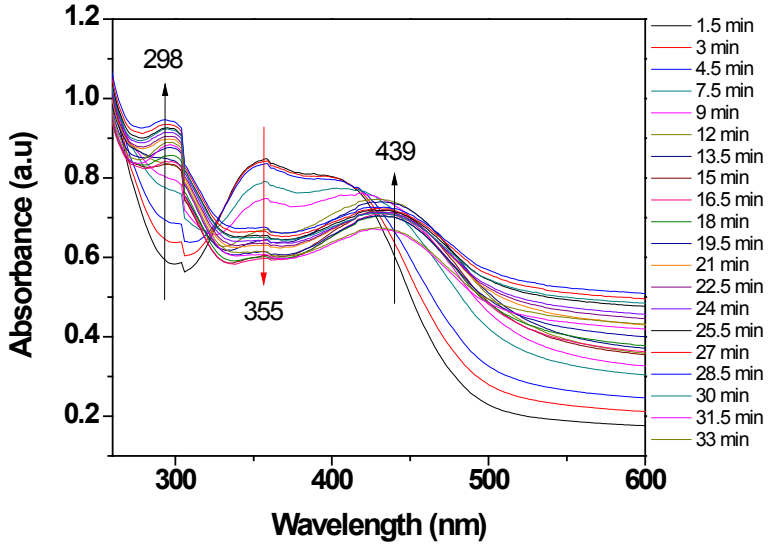

Fig. 7. Time-dependent UV-vis absorption spectrum for the reduction of DNP with $NaBH_4$ in the presence of AgNPs as a catalyst, first 33 minutes.

Thereafter, the absorptions at 439 nm gradually decreased as 2,4-dinitrophenolate intermediate transformed into DAP. Within the next 72 minutes, the absorption bands of the 2,4-dinitrophenolate ion was totally disappeared and spectrum became stable as shown in Fig. 8. The reaction solution became colorless.

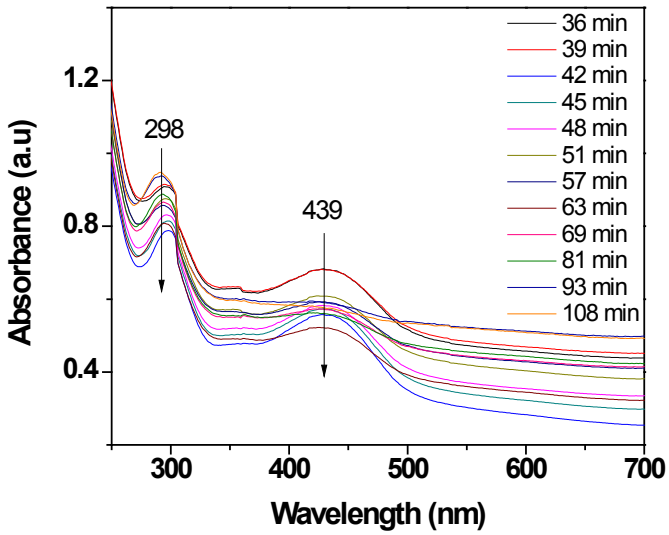

Fig. 8. Time-dependent UV-vis absorption spectrum for the reduction of DNP with $NaBH_4$ in the presence of AgNPs as a catalyst, last 72 minutes.

In order to compare the catalytic activity of the metal nanoparticles, rate constant of the reactions was calculated from the decrease in intensity of the absorption peak at 355 nm over time. As the concentration of sodium borohydride can be considered constant, the change in the ratio lnA with time corresponds to a first-order reaction kinetics equation, and the rate constant can be directly calculated from the linear relation between lnA and time. Fig. 9 shows the kinetic curves of the DNP reduction processes. From these kinetic curves, the rate constants (k, s^{-1}) were found to be 5.00×10^{-6} s^{-1}, 1.24×10^{-2} s^{-1} and 8×10^{-3} s^{-1} for the reaction without any metal nanoparticles, with AuNPs and AgNPs, respectively. By comparing these rate constants of DNP reduction, it can be noted that both metal nanoparticles accelerated the process and showed an excellent catalytic activity.

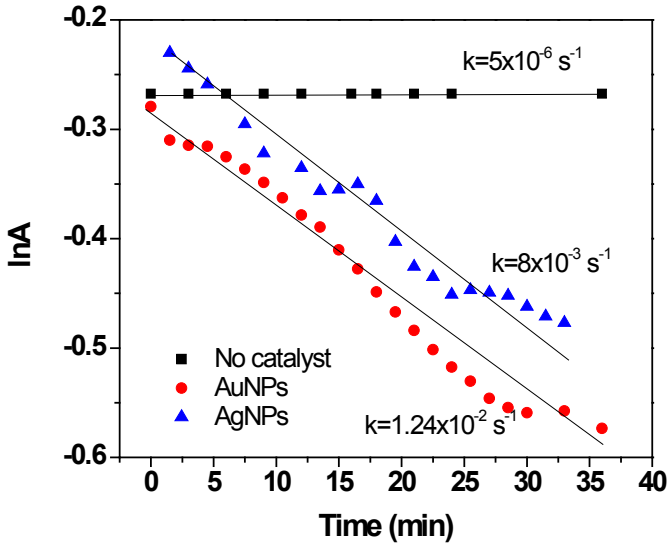

Fig. 9. ln[DNP] versus time plots using no catalyst, gold nanoparticles and silver nanoparticles as catalysts for the reduction of DNP carried out at 25 °C.

Conclusion

The catalytic performance of AuNPs and AgNPs was tested by using UV-vis absorption spectrometer in terms of the catalytic reduction of 2,4-dinitrophenol. From kinetic curves of the reactions, the rate constant (k, s^{-1}) was found to be 5.00×10^{-6} s^{-1} for non-catalyst reaction, while in the presence of AuNPs and AgNPs catalysts, those were 1.24×10^{-2} s^{-1} and 8×10^{-3} s^{-1}, respectively.

Overall results show that as-synthesized AuNPs ans AgNPs have excellent catalytic efficiency in terms of activity and stability in the catalytic reduction of 2,4-dinitrophenol in aqueous sodium borohydride solution under mild conditions.

Acknowledgement

We thank the Asian Research Center Project for the support of this research (2016-1255).

References

[1] C.T. Campbell, The active site in nanoparticle gold catalysis, Science 306 (2004), 234-235.

[2] R.W. Taylor, R. Esteban, S. Mahajan, J. Aizpurua, and J. Baumberg, Optimizing SERS from gold nanoparticle clusters: Addressing the near field by an embedded chain plasmon model, J. Phys. Chem. C 120 (2016), 10512-10522.

[3] Q.L. Cui, F. He, X.Y. Wang, B.H. Xia, and L.D. Li, Gold nanoflower@gelatin core–shell nanoparticles loaded with conjugated polymer applied for cellular imaging, ACS Appl. Mater. Interfaces 5 (2013), 213-219.

[4] X.H. Huang, I.H. El-Sayed, W. Qian, and M.A. El-Sayed, Cancer cells assemble and align gold nanorods conjugated to antibodies to produce highly enhanced, sharp, and polarized surface Raman spectra: a potential cancer diagnostic marker, Nano Lett. 7 (2007), 1591-1597.

[5] X. Huang and M.A. El-Sayed, Gold nanoparticles: Optical properties and implementations in cancer diagnosis and photothermal therapy, J. Advan. Res. 1 (2010), 13-28.

[6] M. Notarianni, K. Vernon, A. Chou, M. Aljada, J. Liu, and N. Motta, Plasmonic effect of gold nanoparticles in organic solar cells, Solar Energy 106 (2014), 23-37.

[7] K.B. Mogensen, K. Kneipp, Size-dependent shifts of plasmon resonance in silver nanoparticle, J. Phys. Chem. C 118 (2014), 28075-28083.

[8] Z.M. Xiu, Q.B. Zhang, H.L. Puppala, V.L. Colvin, and P.J.J. Alvarez, Negligible particle-specific antibacterial activity of silver, Nano Lett. 12 (2012), 4271-4275.

[9] F.A. Cunha, K.R. Maia, E.J.J. Mallman, O. Cunha, A.A.M. Maciel, I.P. Souza, E.A. Menezes, and P.B.A. Fechine, Silver nanoparticles-disk diffusion test against *Escherichia coli* isolates, Rev. Inst. Med. Trop. San Paulo 58 (2016), 73-76.

[10] C.A. Osborne, T.B.D. Endean, and E.R. Jarvo, Silver-catalyzed enantioselective propargylation reactions of n-sulfonylketimines, Org. Lett. 17 (2015), 5340-5343.

[11] C.Y. Chiu, P.J. Chung, K.U. Lao, C.W. Liao, and M.H. Huang, Facet-dependent catalytic activity of gold nanocubes, octahedra, and rhombic dodecahedra toward 4-nitroaniline reduction, J. Phys. Chem. C 116 (2012), 23757-23763.

[12] J. Zeng, Q. Zhang, J. Chen, and Y. Xia, A comparison study of the catalytic properties of Au-based nanocages, nanoboxes, and nanoparticles, Nano Lett. 10 (2010), 30-35.

[13] J. Zhang, Z. Sun, Y. Li, X. Peng, W. Li, and Y. Yan, Biodegradation of p-nitrophenol by *Rhodococcus* sp. CN6 with high cell surface hydrophobicity, J. Hazard. Mater. 163 (2009), 723-728.

[14] S. Saha, A. Pal, S. Kundu, S. Basu, and T. Pal, Photochemical green synthesis of calcium-alginate-stabilized Ag and Au nanoparticles and their catalytic application to 4-nitrophenol reduction, Langmuir, 26 (2010), 2885-2893.

[15] T. Ma, W. Yang, S. Liu, H. Zhang, and F. Liang, A comparison reduction of 4-nitrophenol by gold, Catalysts 7 (2017), 38-48.

[16] F.A. Al-Marhaby, R. Seoudi, Preparation and Characterization of Silver. World Journal of Nano Science and Engineering, 6 (2016) 29-37.

[17] X.-Q. Wu, X.-W. Wu, Q. Huang, J.-S. Shen, H.-W. Zhang, In situ synthesized gold nanoparticles in hydrogels for catalytic reduction of nitroaromatic compounds, Applied Surface Science, 331 (2015), 210-218.

[18] K. Karakas, A. Celebioglu, M. Celebi, and T. Uyar, M. Zahmakiran, Nickel nanoparticles decorated on electrospun polycaprolactone/chitosan nanofibers as flexible, highly active and reusable nanocatalyst in the reduction of nitrophenols under mild conditions, Applied Catalysis B: Environmental, 203 (2017), 549–562.

[19] Erdene-Ochir Ganbold, Simultaneous Monitoring of Adsorbed Simultaneous Monitoring of Adsorbed Nanoparticle Carriers, Doctoral Dissertation. 2013.

[20] Ratyakshi and R.P. Chauhan, Colloidal Synthesis of Silver Nano Particles, Asian Journal of Chemistry. 10 (2009) 113-116.